Synergistic interaction between sensory inputs and propriospinal signalling underlying quadrupedal locomotion

Marie Boulain, Inès Khsime, Mélissa Sourioux, Muriel Thoby-brisson, Grégory Barrière, John Simmers, Didier Morin, Laurent Juvin

Title (108/120 characters)

Synergistic interaction between sensory inputs and propriospinal signaling underlying quadrupedal locomotion

Running Title: Interaction of sensory and central spinal pathways

Author names and affiliation

Marie Boulain, Ines Khsime, Mélissa Sourioux, Muriel Thoby-Brisson, Grégory Barrière, John Simmers, Didier Morin and Laurent Juvin

Univ. Bordeaux, CNRS, EPHE, INCIA, UMR 5287, F-33000 Bordeaux, France

Correspondence should be addressed to:

Laurent Juvin, Institut de Neurosciences Cognitives et Intégratives d'Aquitaine, Unité Mixte de Recherche 5287, Centre National de la Recherche Scientifique, Université de Bordeaux, 33076 Bordeaux, France. laurent.juvin@u-bordeaux.fr

Number of pages: 39

Number of figures: 8

Number of tables: 2

Number of words in the whole manuscript: 7,157

Number of words in the Abstract/Introduction/Discussion: 238/734/3048

Keywords: locomotion, neonatal rodent, neural network interactions, sensory pathways

Additional information section

Data availability statement

All data supporting the results have been included in the manuscript figures.

Competing interests

The authors declare no competing interests.

Author Contributions

LJ, MTB, JS and DM designed research; MB, IK, MS, GB and LJ performed research; IK, MS, LJ and GB analyzed data; MB, IK, MS, MTB, GB, JS, and DM edited the paper; LJ wrote the paper.

All authors approved the final version of the manuscript.

All authors agree to be accountable for all aspects of the work in ensuring that questions related to the accuracy or integrity of any part of the work are appropriately investigated and resolved.

All persons designated as authors qualify for authorship, and all those who qualify for authorship are listed.

Acknowledgements

The present work was partially supported by 'Equipe FRM' funding (DEQ20170336764) to M.T-B. The authors also thank Anne Fayoux for animal care and her management of breeding. The authors are also grateful to Aslak Grinsted for the matlab wavelet coherence package (http://noc.ac.uk/using-science/ crosswavelet-wavelet-coherence) and Philipp Berens for the circular statistics toolbox.

Key Points

-Stimulation of hindlimb afferent fibers can both stabilize and increase the activity of fore- and hindlimbs motoneurons during fictive locomotion.

-The increase in motoneuron activity is at least partially due to the production of doublets of action potentials in a subpopulation of motoneurons.

-These results were obtained using an *in vitro* brainstem/spinal cord preparation of neonatal rat.

Abstract

Quadrupedal locomotion relies on a dynamic coordination between central pattern generators (CPGs) located in the cervical and lumbar spinal cord, and controlling the fore- and hindlimbs, respectively. It is assumed that this CPG interaction is achieved through separate closed-loop processes involving propriospinal and sensory pathways. However, the functional consequences of a concomitant involvement of these different influences on the degree of coordination between the fore- and hindlimb CPGs is still largely unknown. Using an *in vitro* brainstem/spinal cord preparation of neonatal rat, we found that rhythmic, bilaterally-alternating stimulation of hindlimb sensory input pathways elicited coordinated hindlimb and forelimb CPG activity. During pharmacologically-induced fictive locomotion, lumbar dorsal root (DR) stimulation entrained and stabilized an ongoing cervico-lumbar locomotor-like rhythm, and increased the amplitude of both lumbar and cervical ventral root bursting. The increase in cervical burst amplitudes was correlated with the occurrence of doublet action potential firing in a subpopulation of motoneurons, enabling the latter to transition between low and high frequency discharge according to the intensity of DR stimulation. Moreover, our data revealed that propriospinal and sensory pathways act synergistically to strengthen cervico-lumbar interactions. Indeed, split-bath experiments showed that fully coordinated cervico-lumbar fictive locomotion was induced by combining pharmacological stimulation of either the lumbar or cervical CPGs with lumbar DR stimulation. This study thus highlights the powerful interactions between sensory and propriospinal pathways which serve to ensure the coupling of the fore- and hindlimb CPGs for effective quadrupedal locomotion.

Introduction

Quadrupedal locomotion requires a tight coordination between the fore- and hindlimbs whose rhythmic movements need to be regulated in a highly dynamic manner in order to facilitate gait transitions or adaptations to environmental constraints. It is now well established that the locomotor rhythms and movement patterns of the fore- and hindlimbs are generated by distinct spinal cervical and lumbar central pattern generators (CPGs), respectively (Viala and Vidal, 1978; Cazalets et al., 1995; Kjaerulff and Kiehn, 1996; Ballion et al., 2001; Grillner, 2011; Rossignol, 2011; Frigon, 2017). The mechanisms by which these separate locomotor CPGs coordinate their activities therefore appear to be key to understanding how the central nervous system can produce a global and unified motor program underlying a multiple limb behavior.

From the use of *in vivo* approaches, the coordination between the cervical and lumbar CPGs has been shown to rely on three main actors: (1) supraspinal descending pathways to the spinal cord, (2) propriospinal interneurons, and (3) sensory inputs resulting from movements of the limbs themselves (Miller et al., 1975; English, 1979; Matsukawa et al., 1982; Udo et al., 1982; Rossignol et al., 1993; Jordan and Schmidt, 2002; Zaporozhets et al., 2011; Frigon, 2017). However, how the propriospinal pathways interact with sensory inputs in the intraspinal coupling process remains to be elucidated. On one hand, propriospinal interneuronal pathways participate in coupling the fore- and hindlimb CPGs via both long direct and thoracic-relayed indirect connections (Ballion et al., 2001; Juvin et al., 2005; Reed et al., 2006; Ruder et al., 2016). On the other hand, sensory inputs are also key contributors to the regulation of interlimb coordination. For instance, in the spinalized cat, stimulation of limb cutaneous or proprioceptive afferents are known to induce episodes of locomotion, revealing an access of these inputs to the locomotor CPGs (Rossignol et al., 2006). These observations have also been reproduced *in vitro* where the stimulation of hindlimb low threshold proprioceptive inputs activates, in a coordinated manner, the cervical and lumbar CPGs in isolated spinal cord preparations (Marchetti et al., 2001; Juvin et al., 2012).

Furthermore, there is evidence to suggest that propriospinal signaling and sensory inputs do not act independently. It is well established that limb afferent pathways interact not only with local propriospinal circuitry where the afferent fibers enter the spinal cord, but also with circuits located in more remote cord segments. For example, modulation of the soleus H-reflex can occur during rhythmic movement of the forelimb (Frigon et al., 2004; Phadke et al., 2010), therefore suggesting that such a distant action is likely to participate in forelimb/hindlimb coupling during locomotor behavior. Moreover, data from cat has shown that cutaneous afferents elicit interlimb reflexes involving all four limbs, thus also pointing to a role of such inputs in regulating interlimb coordination during locomotion (Hurteau et al., 2018). In high spinal cats, stimulation of forelimb afferent nerves was shown to trigger excitatory post-synaptic potentials in hindlimb motoneurons, further revealing the contribution of

intraspinal circuits in organizing quadrupedal reflexes (Schomburg et al., 1977). Similar observations were also reported in humans, indicating that the principles of organization of the mechanisms ensuring and regulating interlimb coordination are conserved across quadrupeds and bipeds alike (Haridas et al., 2006).

Here, we investigated how an interaction between limb sensory inputs and propriospinal circuits serves as an intraspinal coupling mechanism during locomotion. First, we measured parameters of quadrupedal limb movements during L-DOPA-induced overground- and air-stepping in the neonatal rat. Then, using a brainstem/spinal cord *in vitro* preparation, we combined pharmacological manipulation of the spinal locomotor networks together with alternating bilateral electrical stimulation of dorsal root (DR) afferents to mimic their timing of activation during actual locomotor limb movements. We show that, even at low intensity, such rhythmic stimulus trains delivered to lumbar DRs that mimic phasic afferent inputs *in vivo* can strengthen ongoing fictive locomotion by stabilizing both the rhythms of, and the coupling between, the two CPG circuits. This stimulation protocol increased the amplitude of ventral root discharges that coincide with a transition to high frequency doublet firing by a subpopulation of motoneurons. Moreover, we show that low intensity lumbar DR stimulation can elicit episodes of coordinated cervico-lumbar fictive locomotion when combined with a subthreshold pharmacological stimulation of either the cervical or lumbar CPGs. Our results reveal for the first time how sensory and propriospinal pathway signaling can combine directly to elicit and maintain coordinated CPG network activity appropriate for quadrupedal locomotion.

Materials and Methods

Ethical approval.

All procedures were conducted in accordance with the local ethics committee of the University of Bordeaux (APAFIS#11978-2017103012063751) and the European Communities Council Directive (2010/63/EU). Experiments were performed on newborn (0 to 3 day old) Wistar rats that were obtained from our laboratory's breeding facility. The animals had full access to their mother's milk, and the mothers were fed ad libitum with full access to water. Every effort was made to minimize suffering and the number of animals used.

In vivo locomotion

Animal limb articulations were tagged using reflective face makers (diam 3 mm, optitrack), and injected with a L-DOPA solution (75 mg/kg). Then the animals were either suspended in the air, or put on the ground and filmed at 25 Hz using either a Raspberry Pi or GoPro camera. Tracking of the marker trajectories was achieved using the Kinovea software (https://www.kinovea.org/), and measurements of the angular excursion of the hip (toe-hip-shoulder) and the shoulder (toe-shoulder-hip) were performed using routines written in Matlab software (https://fr.mathworks.com/).

In vitro spinal cord preparations.

Animals were deeply anesthetized by exposure to isoflurane (4%) and decapitated. The skin and muscles were swiftly removed and preparations were then placed in a 25 ml recording chamber containing circulating artificial CSF (ACSF; see composition below). The flow rate was adjusted so as to change the total chamber volume within 5 min. Under a binocular microscope, the spinal cord was then isolated with its dorsal and ventral roots still attached and fixed on a Sylgard resin block with the ventral surface facing upwards. Preparations were superfused continuously with ACSF equilibrated with 95% O_2/5% CO_2, pH 7.4, and containing the following (in mM): 113 NaCl, 4.5 KCl, 1 NaH_2PO_4, 2 $CaCl_2$, 1 $MgCl_2$, 25 $NaHCO_3$ and 11 D-glucose.

For most preparations, the recording chamber was partitioned into two compartments with independent perfusion systems. Narrow petroleum jelly bridges allowed the cord to remain functionally intact between the compartments, and water tightness was checked at the end of each experiment by observing the movements of methylene blue dye added to the bathing medium on either side of a given bridge.

Electrophysiological recording and electrical stimulation.

A transverse section of the spinal cord was performed at the C7 level, then the cervical part of the cord was placed on an inclined surface such that the cut C7 segment paralleled the surface of the bath. In this way, with this so-called "retroussée" preparation, the C7 segment was oriented in a manner equivalent to a coronal slice, providing direct access to the cervical motoneurons (Beliez et al., 2015).

Whole-cell configuration recordings in current clamp mode were made using an Axoclamp 2B amplifier (Molecular Devices). Antidromic action potentials elicited by brief pulse electrical stimulation of the corresponding ventral root were used to identify recorded cells as motoneurons (Fig. 4B). Only motoneurons whose membrane potential remained at a stable resting potential of at least -50mV were investigated further. Patch clamp micropipettes (3-5MΩ) were filled with the following intracellular solution (in mM): 120 K-gluconate ; 0.1 $CaCl_2$; 0.1 $MgCl_2$; 1 EGTA ; 3 Na_2-ATP ; 10 HEPES ; 77 D-Mannitol ; 0.1 GTP ; 0.2 cAMP ; 0.1 Leupeptin ; 1% Biocytine, with the pH adjusted to 7.2 and osmolarity to 306 mOsm.

Motor output activity in spinal ventral roots was recorded using glass suction electrodes. Signals were amplified (10,000x) by differential AC amplifiers (low cutoff, 100 Hz; high cutoff, 1 kHz; model 1700, A-M Systems), digitized and acquired via a CED1401 interface, stored on a computer, and analyzed using Spike2 software (Cambridge Electronic Design). Electrical pulse train stimulation over an amplitude range of 0.5 to 3V at 0.3 ms per pulse and 5 Hz was applied to spinal dorsal roots (DRs) via glass suction electrodes using an eight-channel digital stimulator (A.M.P.I.). For each preparation, the stimulus threshold to elicit fictive locomotion (LocoTh) was determined by progressively increasing the intensity of the DR stimulations.

Drug application.

Pharmacological substances were bath-applied, beginning at a minimum of 30 min after the end of dissection. A mixture of N-methyl-D,L-aspartate (NMDA; 3.75-7.5 µM), serotonin (5-HT; 7.5-15 µM) (both purchased from Sigma) was used to elicit prolonged and stable episodes of fictive locomotion (Kudo and Yamada, 1987; Smith and Feldman, 1987; Cazalets et al., 1992). In some experiments, the partitioning of the recording chamber into two compartments with a barrier of syringe-ejected Vaseline (see above) allowed the differential exposure of selected spinal cord regions to pharmacological stimulation. In other cases, a modified ACSF containing a lowered Ca^{2+} concentration (0.1 mM $CaCl_2$, 5 mM $MgCl_2$) was bath-applied to the lumbar compartment to reversibly block chemical synaptic transmission within that cord region.

Data analysis.

The coordination between the burst activities of different spinal ventral roots was examined by means of cross-correlation analysis. The phase relationship between locomotor bursts in different ventral roots was determined by constructing a circular phase diagram from normalized cycles (Kjaerulff and Kiehn, 1996). In each experiment, bursts of a given ventral root (VR1) were randomly selected from a sequence of stable rhythmic activity and taken as the reference. The phase values of burst onsets in a second ventral root (VR2) with respect to VR1 were determined by dividing the latency from the start of each VR1 burst to the next VR2 burst onset by the VR1 cycle period. The phase values were then plotted on a circular phase diagram with a scale ranging from 0 to 1, where values close to 0.5 reflected

burst alternation, and values approaching 0 or 1 indicated phase coincidence. This provided a mean vector whose direction and length (r, also on a scale of 0 to 1) indicated, respectively, the preferred phase and strength of phase coupling between bursts in the selected nerve pairs. The evaluation of r, using the Rayleigh test to determine the concentration of phase values around the mean vector, estimated the coupling strength (considered to be significant for $p < 0.05$).

Cross-coherence maps of ventral root activities were performed using wavelet transform analyses provided by Aslak Grinsted (http://noc.ac.uk/using-science/crosswavelet-wavelet-coherence). A detailed explanation of the wavelet-based methodology used in the present work has been previously reported (Mor and Lev-Tov, 2007; Beliez et al., 2015). Average traces of rectified and integrated recordings obtained by averaging at least 20s of fictive locomotion were used to compare fictive locomotion evoked by the different stimulation protocols employed. Maximal amplitudes of impulse bursts were compared when fictive locomotion was evoked either by pharmacological activation alone or when pharmacological activation was combined with electrical stimulations of DR roots. Group values were expressed as means +/- SD, with (n) referring to the number of animals used. Differences between means were analyzed using SigmaPlot 11.0 (Systat) and assessed by Student's paired t-test, or either a one-way ANOVA and Tuckey *post hoc* tests. A one way ANOVA on ranks and Dunn's *post hoc* tests were used when more than 2 groups were compared. Differences in mean values for each parameter were taken to be significant at $p < 0.05$.

Results

Inter-appendicular coupling during locomotion relies on limb sensory feedback

Overground locomotion or air-stepping can be triggered by the injection of L-DOPA (75 mg/kg) in the neonatal rat (McCrea et al., 1994). Whether the animal was in direct contact with the ground (Fig. 1A) or suspended in the air (Fig. 1C), both the fore- and hindlimbs displayed rhythmical alternating movements in response to L-DOPA injection (Fig. 1B and D). During overground locomotion, the locomotor cycle frequency measured from the fore- and hindlimbs remained closely correlated (forelimbs: 0.20 +/- 0.02 Hz, hindlimbs 0.20 +/- 0.04 Hz; Fig. 1E). In contrast, during air-stepping, the mean frequency of the forelimb locomotor movements was overall faster than that of the hindlimbs (2.10 +/- 0.59 Hz vs 1.46 +/- 0.17 Hz; Fig. 1F). However, most of the time (61.56% of cycles) these periods remained sufficiently close for a 1:1 coupling (one forelimb step per hindlimb step) to occur. For the remaining cycles, the forelimb/hindlimb periods differed in such a way that other coupling values, different from pure harmonics, emerged. This directly altered the global quality of the anteroposterior interlimb coupling during air-stepping compared to overground locomotion (forelimb/hindlimb 1:1 coupling: 61.56 +/- 23.79 % vs 100%; Fig. 1G), which was also confirmed using the Rayleigh distribution analysis of the homolateral forelimb/hindlimb phase relationships (0.88 +/- 0.18 vs 0.50 +/- 0.24; Fig. 1H).

It should be noted that during air-stepping, since there is no ground contact, there no weight support during each stance phase. This necessarily reduces the activation of foot cutaneous afferents, and also limits the spatio-temporal activation pattern of proprioceptive inputs carrying loading/unloading information, as well as muscle contraction/stretching levels from the different joints. Given the importance of these inputs in controlling phase transitions during overground locomotion (Hiebert et al., 1996; Hiebert and Pearson, 1999; Rossignol et al., 2006), this may at least partly explain the reduced angular excursion of the limb observed during air-stepping and the variability observed in antero/posterior coupling.

Fictive quadrupedal locomotion induced by combined dorsal root and pharmacological stimulations

Episodes of fictive quadrupedal locomotion in brainstem/spinal cord preparations of the neonatal rat can be induced by rhythmic bilateral stimulation of the second lumbar (L2) dorsal root (DR) afferents (Juvin et al., 2007, 2012). In the present study, stimulus trains (0.3 ms pulses at 5 Hz for 2 s and repeating every 4 s) were delivered alternately to the left and right lumbar L2 dorsal roots in otherwise quiescent preparations under normal ACSF exposure. First, in all tested preparations we determined the minimal stimulation intensity (locomotor threshold, LocoTh) required to elicit fictive locomotion

by progressively increasing the intensity of the DR stimulations (Fig. 2A and 3E). It is noteworthy that in our experiments, LocoTh was found to be about twice the minimal stimulation intensity required to trigger a monosynaptic reflex response in the ventral root of the same cord segment as the stimulated DR (Fig. 3E; Juvin et al., 2012). Simultaneously, any locomotor-like activity expressed was monitored by bilateral extracellular recordings from the cervical (C8) and lumbar (L2) ventral roots that normally innervate forelimb extensor muscles and hindlimb flexor muscles, respectively (Fig. 2A). As reported previously, such induced activity was strictly timed to the rhythm imposed by the DR stimulation protocol (Juvin et al., 2007), with activity phase relationships that corresponded to quadrupedal walking *in vivo* (Ballion et al., 2001; Juvin et al., 2005). Thus, bilateral burst alternation occurred at each of lumbar and cervical segmental levels (Fig. 2A right; Table 1 and 2), while bursting in homolateral C8/L2 ventral roots were expressed in synchrony.

As previously reported (Cazalets et al., 1992), the perfusion of a mixture of NMDA (7.5 µM) and 5-HT (15 µM) over these *in vitro* preparations (Fig. 2B, left) also elicits episodes of fictive locomotion (Fig. 2B, left segments of traces; Table 1 and 2), characterized by a stable rhythm period of 5.13 +/- 1.05 s (n = 9; Table 1). We next performed a combined stimulation protocol (CSP) that consisted of delivering bilaterally-alternating stimulus trains with a cycle period of 4 s to the L2 DRs during such pharmacologically-induced fictive locomotion. During CSP, the ongoing quadrupedal locomotor-like pattern became strictly coordinated with the rhythm imposed by the DR stimulations (3.98 +/- 0.06 s; n = 9; Fig. 2B, right and C; Table 1), and the variability of the rhythm was reduced, as indicated by the significant reduction in the coefficient of variation of the rhythm's cycle period (0.2 vs 0.02; see Table 1). However, the phase relationships between the spinal ventral root burst activities were not significantly different ($p = 0.275$; Table 2) whether the CPG rhythm was induced by NMDA/5-HT alone or in combination with DR stimulations (Fig. 2D). Thus, alternating bilateral stimulation of lumbar DRs is able to entrain and stabilize the rhythm period of ongoing pharmacologically-induced quadrupedal fictive locomotion.

Convergent interaction between propriospinal and sensory ascending pathways

In addition to the remote influence of sensory feedback from the hindlimbs, as described above (Juvin et al., 2012) the cervical CPG networks can be activated via propriospinal pathways that interconnect the lumbar and cervical CPGs via thoracic segmental relays (Juvin et al., 2005). However, the extent to which these parallel ascending inputs cooperate to ensure cervico-lumbar coordination during quadrupedal locomotion remains undetermined. To address this issue, we performed a series of experiments in which a Vaseline bridge was placed at the mid-thoracic (T7) cord level to enable exposure of the lumbar and cervical CPGs to different pharmacological conditions.

First, in quiescent preparations bathed in normal ACSF, stimulations were delivered to the left and right L2 DRs at intensities that were below the threshold (LocoTh) for triggering fictive locomotion, and were thus defined as sub-locomotor threshold (SubLocoTh) stimulations (Fig. 3A). At these intensities, none of the preparations expressed fictive locomotor activity, either at the cervical or at the lumbar levels (n = 0/7; Fig. 3A). In a second step, to activate ascending propriospinal neurons by the lumbar CPGs, a mixture of NMDA (7.5 µM) and 5-HT (15 µM) was perfused over the low thoraco-lumbar segments (Fig. 3B). Under this condition, locomotor-like activity was now expressed in the lumbar but still not the cervical cord regions (n = 7/7; Fig. 3B, left), indicating that the propagation of lumbar CPG-related activity in ascending propriospinal neurons was alone insufficient to evoke cervical CPG activation (see also Juvin et al. 2005). However, when pharmacological activation of the lumbar CPGs was now combined with bilateral SubLocoTh L2 DR stimulation (Fig. 3B, right), the ongoing lumbar rhythm increased in amplitude and its cycle period became stabilized compared to pharmacological activation alone (CV = 0.21 vs 0.03; Table 1). Importantly, moreover, strongly coordinated cervico-lumbar locomotor-like activity now occurred (n = 7/7), which consisted of alternating bilateral burst activities at the lumbar and cervical levels, and synchronous bursting between homolateral C8 and L2 ventral roots (Fig. 3B, right; Table 2). These findings are thus consistent with the conclusion that pharmacologically-induced activation of ascending propriospinal neurons combine with low intensity (SubLocoTh) stimulation of lumbar DRs to provide an additional excitation that ultimately leads to the expression of coordinated fictive quadrupedal locomotion.

A question that immediately arises is whether hindlimb afferent inputs produced by SubLocoTh lumbar DR stimulation are able to reach the cervical locomotor networks without requiring activation of the lumbar locomotor circuitry. To resolve this issue, we stimulated the lumbar DRs with SubLocoTh intensities during the perfusion of a cocktail of NMDA (3.75 µM) and 5-HT (7.5 µM) applied exclusively to the cervical segments (Fig. 3C). It is important to note that at these concentrations, the NMDA/5-HT cocktail alone did not induce any locomotor-related activity (Fig 3C). However, under this condition (n= 9/9 preparations), robust rhythmic bursting was evoked at the cervical level when the L2 dorsal roots were alternately stimulated (Fig. 3C), whereas in all cases, locomotor-related activity was absent in lumbar ventral roots. On the other hand, when the same SubLocoTh L2 DR stimulation protocol was applied in combination with a low concentration NMDA/5-HT cocktail perfused either selectively at the lumbar level or over the whole spinal cord, the bilateral sensory pathway activation was now sufficient to trigger fictive quadrupedal locomotion (Fig. 3E). Together these experiments indicated that the presence of the subthreshold pharmacological stimulation effectively lowered the intensity of DR stimulations required to activate the spinal locomotor circuits by 29.5%.

Finally, to assess the extent to which the lumbar DR-cervical influence is transmitted by long direct connectivity rather than indirectly via lumbar CPG circuitry, we blocked lumbar polysynaptic

pathways using a modified (low calcium/high magnesium) aCSF applied locally to the caudal cord region, while the rostral cord was exposed to low concentration (3.75/7.5 µM) NMDA/5-HT (Fig. 3D). Under these conditions, L2 DR stimulation failed to induce any lumbar locomotor-related activity, but could still activate the cervical CPG in 6 out of 7 preparations (85.7%). In these experiments, however, the blockade of lumbar circuit synapses was found to increase the DR stimulus threshold for locomotor-like activity induction by an average of 25.6% (n = 6; p = 0.013; Fig. 3E). This finding therefore indicates that despite the ability of predominantly direct projection pathways to activate the cervical locomotor networks, a significant indirect DR afferent influence conveyed in parallel via lumbar circuitry and, in turn, ascending propriospinal pathways also plays an important role in activating the cervical CPG.

Remote influence of lumbar sensory inputs on cervical motoneurons

Given that lumbar DR activation clearly has access to the CPG circuitry that generates forelimb motor bursting, in a next series of experiments, we sought how this remote afferent influence impacts on the responsiveness of individual cervical motoneurons. To this end, intracellular recordings were made from identified cervical motoneurons in so-called “retroussée” preparations (n = 7), with spinal segments more rostral to C7 removed to enable patch clamp recording (see Materials and Methods) during L2 DR stimulation alone (Fig. 4A) or in combination with pharmacological activation (see Fig. 5). These single recorded neurons (n = 7), whose axons were confirmed to project in the ipsilateral C7 ventral root that innervates forelimb extensor muscles *in vivo* (Fig. 4B), displayed rhythmic oscillations in membrane potential and impulse bursting that were clearly related to fictive quadrupedal locomotion (Fig. 4C). Accordingly, these oscillations and burst discharge in individual C7 motoneurons occurred in phase with burst activity in the ipsilateral C7 ventral root and in phase opposition with bursting in both the contralateral C7 and L2 ventral roots.

Important features of the sensory pathway-derived influence conveyed from the lumbar to cervical spinal regions were evident from the responses of patch clamp recorded C7 motoneurons both to single electrical shocks (Fig. 4D) or alternating train stimulation (Fig. 4F) of increasing intensities (from 0.5 up to 2.5V) delivered to the ipsilateral L2 DR or to the left and right L2 DRs, respectively. Single DR pulse stimulation evoked EPSPs in individual C7 motoneurons, of which the first synaptic responses occurred at constant latency (mean 52.03 +/- 6.21 ms, Fig. 4D) and summated with increasing stimulus intensities. Despite the strict 1:1 occurrence of these initial post-stimulus EPSPs and a low CV value (0.02) of the delay between the EPSPs and the stimulation, a significant jitter of 1.14 +/- 1.38 ms was nonetheless observed. Taken together, our results strongly suggest the involvement of a relayed but reliable synaptic pathway in signal transmission from the lumbar dorsal roots to C7 motoneurons. When stimulation trains of increasing intensities were delivered alternately

to both L2 DRs, C7 motoneurons were depolarized by a barrage of synaptic excitation associated with rhythmic fluctuations in membrane potential occurring in time with the ipsilateral DR stimulus cycle (Fig. 4F). With increasing stimulus voltages, the synaptic drive to motoneurons correspondingly increased until the thresholds for both impulse firing and cervical CPG network activation were reached, eventually leading to regular burst firing on the depolarized peak of each synaptically-driven oscillation. Our results suggest that even when stimulated at low intensities, the lumbar dorsal roots have a relayed polysynaptic access in the cervical segments to both the locomotor CPG and motoneurons, providing synaptic excitation that acts in synergy with the lumbar CPG network output when DR input becomes sufficient to initiate cervico-lumbar locomotor activity.

Modulation of locomotor CPG activity by lumbar sensory inputs

Next, we investigated the ability of subthreshold stimulation (SubLocoTh) of bilateral lumbar DRs to modulate already ongoing fictive quadrupedal locomotion that was pharmacologically induced by the bath perfusion of NMDA and 5-HT at concentrations of 7.5 µM and 15 µM, respectively (Fig. 5A). Alternating SubLocoTh L2 DR stimulation modulated the drug-induced locomotor rhythm by imposing the stimuli trains own 4 s cycle period (4.04 +/- 0.35 s; n = 7; Fig. 5B; Table 1), which also became stabilized as attested to by the reduction in the rhythm period's coefficient of variation (0.2 vs 0.09; Table 1). Once again, the phase relationships between the ongoing cervical and lumbar activities were unaltered by the additional lumbar DR stimulation (Fig. 5C; Table 2), and indeed, spectral coherence analysis (see Materials and Methods) revealed that the temporal coordination between the two CPGs was considerably strengthened. In comparison to NMDA/5-HT-induced fictive locomotion alone, the coherence value for rC8 vs lL2 activities was significantly increased when pharmacological activation and DR simulations were combined (0.82 +/- 0.06 vs. 0.94 +/- 0.02; n = 7; p = 0.002; Fig. 5D, E). This coordination enhancement appeared early at the onset of DR stimulation and ceased immediately when the stimulation ended (Fig. 5F). Moreover, the coherence modulation was also accompanied by a significant increase in the amplitude of both cervical and lumbar locomotor bursts, as seen in Fig. 5A, G, H where, in the 7 preparations tested, burst amplitudes increased by nearly 300% (100.0 +/- 56.94 % vs. 295.2 +/- 118.58 %; n = 7; p = 0.031). It is noteworthy that similar observations were made for cervical C8 ventral root activity during application of this CSP, further attesting to the ability of sensory information originating from the hindlimbs to remotely modulate excitability levels of the forelimb locomotor network (Fig. 5A, right). Indeed, such a modulation of the amplitude of C8 ventral root bursts is indicative of a direct access of the limb afferent ascending pathways to cervical motoneurons. Taken together, therefore, these results indicate that compared to pharmacological activation alone, CSP involving even low intensity (SubLocoTh) limb afferent stimulation can reliably produce a robust and coordinated cervico-lumbar burst pattern appropriate

for quadrupedal locomotion. Specifically, this combined influence consists of increasing the amplitude of flexor- and extensor-related motor bursting activities, stabilizing the ongoing locomotor-like rhythm, and enhancing the coordination between the fore- and hindlimb CPGs.

In a next series of experiments, the activity of individual C7 motoneurons (n = 6) and cervico-lumbar ventral roots were recorded simultaneously during fictive locomotion induced pharmacologically and subsequently during application of CSP (Fig. 6A). During NMDA/5-HT-induced locomotor activity alone, C7 motoneurons again displayed rhythmic fluctuations in their membrane potential that were coordinated with locomotor burst activity expressed in ventral roots (Fig. 6B, left; 6C). Specifically, the motoneuron oscillations were in phase with both ipsilateral C7 and L2 ventral roots, and in phase-opposition with contralateral C7 and L2 ventral roots (Fig. 6D, top). When a CSP was now applied, the phase relationships between the burst activity of C7 motoneurons and the same ventral roots remained unaltered (Fig. 6D, bottom). However, as seen previously (Fig. 5G, H), in comparison to pharmacological activation alone, the CSP caused a considerable overall increase in the amplitude of the flexor- and extensor-related bursting. This amplitude enhancement was associated with a significant increase (227.77 +/- 114.93 %) in the mean firing frequency of individual C7 motoneurons (3.04 +/- 0.62 Hz), in comparison to pharmacological activation alone (1.34 +/- 1.54 Hz; n = 6; p = 0.032; Fig. 6E). These results indicate that individual cervical motoneurons are similarly activated during either pharmacologically- or remote sensory pathway evoked-modes of fictive locomotion induction. Additionally, when lumbar afferent pathway stimulation is combined with pharmacological locomotor activation, the ensuing increase in cervical ventral root locomotor burst amplitudes is at least partly attributable to an increase in the mean firing frequency of individual cervical motoneurons.

Differential responsiveness of cervical motoneurons to sensory pathway stimulation

In preparations under normal saline conditions (Fig. 7A), two types of C7 motoneurons could be distinguished on the basis of their firing responses to repeated single electrical shocks applied to the ipsilateral L2 DR. In response to DR stimulations delivered at LocoTh intensity, out of 10 patch clamp-recorded motoneurons examined, 5 cells discharged solely a unitary impulse (classified as ‘single action potential motoneurons’ (s.a.Mn); Fig. 7B, C), whereas the remaining 5 neurons constantly expressed doublets of action potentials to the same single pulse stimulation (d.a.Mn; Fig. 7D, E). When fictive locomotion was induced by bilateral LocoTh L2 DR stimulation, both s.a.Mn. and d.a.Mn. displayed membrane potential oscillations and impulse burst firing that were phase-coupled with ipsilateral C7 ventral root activities (Fig. 7F, J). However, the temporal structure of this burst discharge was different for the two types of motoneuron. During DR stimulation-evoked bursts in s.a.Mn., the instantaneous frequencies of action potentials were grouped into an homogenous, relatively low

frequency band (2.92 +/- 0.86 Hz; Fig. 7G, L), in a manner similar to that observed during pharmacologically-induced fictive locomotion (Fig. 7H) and CSP (Fig. 7I). On the other hand, the firing frequencies of d.a.Mn. during DR-evoked bursts were distributed in two distinct low (4.87 +/- 0.53 Hz; Fig. 7K, L) and high frequency domains (63.18 +/- 12.26 Hz; Fig. 7K, L). This difference in burst structure, which was due to the d.a.Mn's capacity to fire doublets in response to individual intra-train stimuli, albeit also observable during CSP (Fig. 7N), was all the more unexpected given that d.a.Mn. discharge was similar to that of s.a.Mn. during pharmacologically-induced fictive locomotion (Fig. 7M), when both motoneuron types expressed impulses solely in the low frequency domain (2.64 +/- 1.59 Hz). Together these results suggest that when alternating lumbar DR stimulation is combined with a pharmacological locomotor activation, the increase in ventral root burst amplitudes is still further augmented by the production of higher frequency action potentials by a subpopulation of cervical motoneurons.

Discussion

Here, we report that in the isolated newborn rat spinal cord, applying bilaterally-alternating hindlimb afferent stimulations to approximate the phasic modulation of limb sensory inputs during actual locomotion (Prochazka and Gorassini, 1998; Taylor et al., 2000), enhances ventral root bursting and increases the coordination between the cervical and lumbar locomotor CPGs (Fig. 8a). Moreover, even at low stimulus intensities, such patterned sensory pathway activation can combine additively with the effects of subthreshold pharmacological stimulation (by a mixture of NMDA/5-HT), to elicit robust locomotor-like activity. This was observed independently of the region exposed to NMDA/5-HT, i.e., whether applied to the cervical or lumbar CPGs, or the whole spinal cord. Notwithstanding the possibility that such processes occurring in a still immature neonate may change in adulthood, our results indicate that sensory and propriospinal pathway signaling (Fig. 8a,b, green and blue lines, respectively) can mutually enhance each other, thereby ensuring the production of strongly coordinated quadrupedal locomotor activity. Additionally, during pharmacologically-induced fictive locomotion, stimulation of hindlimb afferents was found to significantly increase the firing frequency of ~50% of individually recorded forelimb motoneurons (see doublet firing in Fig. 8c), commensurate with a global increase in locomotor burst amplitudes at both lumbar and cervical ventral root levels.

Induction of locomotion by dorsal root stimulation

Induction of locomotor movements by limb afferent stimulation has been long established in the cat and rabbit (Sherrington, 1910; Viala and Buser, 1969), as well as in non-mammalian species such as the lamprey where mechanical stimulation of the tail skin elicits locomotion through the recruitment of primary afferent fibers (Di Prisco et al., 1997). Similar results have also been obtained across various species using epidural stimulation of the dorsal part of the spinal cord, such as in the cat (Iwahara et al., 1992; Barthélemy et al., 2006, 2007), rat (van den Brand et al., 2012) and non-human primates (Capogrosso et al., 2016), and has been used as a powerful tool for re-activating the locomotor centers of spinal cord-injured patients (Dimitrijevic et al., 1998; Herman et al., 2002; Wagner et al., 2018). In a related manner, in the isolated *in vitro* limb-attached brainstem/spinal cord preparation of neonatal rat, stimulation of the dorsal columns of the lumbar spinal cord was shown to elicit episodes of hindlimb locomotor-like movements (Iwahara et al., 1991). In a similar preparation, locomotor-like activity can be elicited either by pinching the tail skin or by delivering electrical stimulation to the sacral DRs (Smith et al., 1988; Marchetti et al., 2001; Juvin et al., 2012). The type of sensory fiber involved in the initiation of locomotion may differ according to the experimental strategy used as, for example, the activation of flexor reflex afferents in the spinalized cat (Jankowska et al., 1967; Grillner, 1969), or low threshold proprioceptive fibers arising from muscle spindles or Golgi tendon organs as was the

case in *in vitro* neonatal preparations (Kudo and Yamada, 1987; Iizuka et al., 1997; Morin and Viala, 2002).

The stimulation protocol used in the present work was partly based on that described in previous studies (Morin and Viala, 2002; Giraudin et al., 2008). From these studies, it is clear that the activation of large-diameter DR axons, which include proprioceptive fibers, in isolated neonatal rat *in vitro* preparations requires relatively low stimulus intensities. The classification of DR afferents as "low threshold" derived from experiments where a proximally placed recording electrode was used to detect the threshold (Th) for *en pass*ant DR impulses elicited by a more distal afferent nerve stimulation (Kiehn et al., 1992; Juvin et al., 2012). In the neonatal rat preparation, stimulation of an L2 DR can reset ongoing fictive locomotion with a stimulus intensity less than 2x the threshold level for producing the incoming volley, implicating a preferential recruitment and involvement of primary afferent fibers (Kiehn et al., 1992). Moreover, in this latter study, the resetting of locomotor activity was achieved through an excitation of L2 (flexor-like) and an inhibition of L5 (extensor-like) motoneurons, which was very similar to the observations made when stimulating either tibialis anterior type II or iliopsoas type Ia afferents in the decerebrate cat (Hiebert et al., 1996). Given the immaturity of our experimental model (Fitzgerald et al., 1987), and the range of stimulation intensities used, we cannot rule out the possibility that smaller diameter fibers and/or fibers arising from cutaneous receptors were also activated and thus contributed to the effects we observed. Indeed, cutaneous inputs also play a key role in adjusting ongoing locomotor patterns, for instance, by correcting the trajectory or the position of the limbs in response to external perturbations (Rossignol et al., 2006). Indeed, their activation during locomotion may lead to a wide variety of multi-limb adjustments that are highly dependent on the state (posture, locomotor phase) of the animal (Frigon et al., 2004; Frigon and Rossignol, 2006; Nakajima et al., 2013).

Influence of sensory feedback on pharmacologically-induced fictive locomotion

Here, we also show that alternating stimulation of bilateral lumbar DRs can modulate the frequency of ongoing fictive locomotion (Fig. 2). Even if the locomotor CPGs can integrate apparently incoherent inputs, as is the case with tonic dorsal root stimulation for instance, during which the networks still generate a locomotor activity (Taccola, 2011; Juvin et al., 2012), Taccola (2011) showed that this was no longer the case when an incoherent sinusoidal stimulation protocol was applied to sensory pathways impinging on the locomotor CPGs. This in turn illustrates the fact that regulating the activity of the locomotor CPGs with afferent inputs requires a coherence between the incoming information and the motor outputs it generates/shapes.

As previously observed in the cat, where resetting of fictive locomotion can be achieved with low intensity stimulation of the tibialis anterior nerve (Perreault et al., 1995), low intensity stimulation of limb afferent pathways in isolated *in vitro* spinal cord preparations of the neonatal rat can also reset and strongly modulate the ongoing activity of the hindlimb locomotor CPGs. In earlier resetting experiments, a brief 20Hz stimulation of the L2 or L3 DR was found to decrease the locomotor cycle period when applied during the extensor-related phase of NMDA/5-HT-induced fictive locomotion (Kiehn et al., 1992). However, this study reported a failure of L5 DR stimulation to reset the fictive locomotor rhythm, suggesting a preferential access of the L2 and L3 DR pathways to the hindlimb locomotor CPGs. On the contrary, a high frequency (75Hz) phasic stimulation of an L4 DR was found to reset the ongoing rhythm (Sqalli-Houssaini et al., 1993), indicating that to be effective, the electrical stimulation of lumbar DRs may require frequency and intensity ranges that are specific for each spinal level.

We found that patterned DR stimulation increases the stability of pharmacologically-induced fictive locomotion and increases the amplitude of ventral root impulse bursts (Fig. 4). Previous studies have reported equivalent results using either a similar mixture of NMDA and 5-HT (Dose and Taccola, 2012), or oxytocin at nanomolar concentrations (Dose et al., 2014). It was proposed that the increase in amplitude of ventral root bursts was due to the recruitment of new populations of motoneurons, as observed in the adult cat (Henneman, 1957) and zebrafish (McLean et al., 2007; Dose and Taccola, 2012). Currently, we cannot exclude the possibility that the increase in ventral root burst amplitude observed in our neonatal preparation is also partly due to the additional recruitment of limb motoneuronal populations. In zebrafish, moreover, a specific pre-motor neuronal population (i.e. V2a interneurons) are recruited depending on locomotion intensity, and in turn activates either slow or fast motoneurons (Ampatzis et al., 2014; Song et al., 2018). Whether a similar functional organization exists in mammals is still unknown, despite the recent identification of 2 distinct populations of V2a interneurons in the mouse spinal cord (Hayashi et al., 2018). Indeed, previous observations in mice showed that pre-motor neurons such as V2a mainly display a steady increase in their firing frequency as locomotor rhythm frequency increases (Zhong et al., 2011). Also, the differential recruitment of separate motoneuron populations has hitherto not been reported in *in vitro* preparations of neonatal rodents where, during pharmacologically-induced episodes of fictive locomotion, individual motoneurons typically discharge at relatively low frequencies (MacLean et al., 1997; Bertrand and Cazalets, 1998; Hochman and Schmidt, 1998). Here, we found that 50% of recorded cervical motoneurons expressed substantially increased firing frequencies in response to lumbar DR stimulation, discharging both in distinct low and high frequency bands (Figs. 6, 7). High frequency doublet firing was initially observed in motoneurons recorded in the cat and humans (Eccles et al., 1932; Denslow, 1948). In humans, these doublets have been found to occur either in response to

548 sensory stimulation or during the initiation of voluntary movements (Kudina and Andreeva, 2013;
549 Mrówczyński et al., 2015). The same phenomenon was also described in the cat at the beginning of
550 motoneuronal burst discharges during actual and fictive locomotion, as well as during fictive scratching
551 (Zajac and Young, 1980; Duenas-Jimenez et al., 2017). High frequency impulse doublets occurring in
552 motoneurons at the beginning of a muscle contraction are associated with a non-linear increase in the
553 contractile (output) strength produced by the muscle fibers. This motoneuronal property, referred to
554 as 'catch' or 'catch-like' property (Burke et al., 1970; Binder-Macleod and Kesar, 2005), has also been
555 reported in invertebrate species (Wilson and Larimer, 1968), and thus appears to be a ubiquitous
556 mechanism by which muscle force levels can be rapidly increased at the onset of a movement.
557
558 **Interactions between propriospinal and sensory signaling pathways**
559 The forelimb and hindlimb locomotor networks of rodents, at least, are known to be interconnected
560 centrally by both long projecting and relayed propriospinal pathways that necessarily mediate the
561 cervico-lumbar CPG coupling observed in the isolated spinal cord under pharmacological activation
562 (Juvin et al., 2005; Ruder et al., 2016). Although peripheral inputs from hindlimb proprioceptors can
563 also activate in a coordinated manner both the cervical and lumbar CPGs, the precise functional
564 relationship that must exist between propriospinal and proprioceptive pathway signaling has remained
565 unclear (Dose and Taccola, 2012; Juvin et al., 2012). Here, we show that stimulation of lumbar DRs
566 stabilizes an ongoing locomotor rhythm and increases the coupling between cervical and lumbar CPG
567 activities (Fig. 5). These findings are strikingly similar to those reported during locomotion in humans,
568 where the interactions between arm and leg movements are enhanced by the stimulation of
569 cutaneous inputs arising from the hands (Zehr et al., 2007). Moreover, several studies have indicated
570 that ensuring interlimb coordination during locomotion in humans also requires the activation of
571 propriospinal circuitry involving direct pathway connections between the cervical and lumbar spinal
572 regions (Dietz, 2002; Frigon, 2017). The finding that activation of the legs CPGs in a cycling task can
573 remotely modulate reflex activity of arm muscles in a phase-dependent-manner, and vice-versa,
574 further strengthens the idea of a strong and direct neuronal link between cervical and lumbar elements
575 (Zehr et al., 2009, 2016).
576 Finally, locomotor CPG output *in vivo* may be further enhanced by other co-operative signaling
577 interactions, such as those existing between ascending propriospinal pathways and descending fibers
578 originating from the medullary reticular formation (Oueghlani et al., 2018). Indeed, the reticular
579 formation contains neurons whose activity is correlated with the activation of different forelimb
580 and/or hindlimb muscles (Perreault et al., 1993; Matsuyama and Drew, 2000). In addition, complex
581 inter-limb motor responses can be evoked by microstimulations of the medullary reticular formation
582 in the cat during actual and fictive locomotor episodes (Drew and Rossignol, 1990a, 1990b; Perreault

et al., 1994). Thus, under normal conditions, limb sensory inputs could contribute indirectly to coordinating cervical and lumbar motor outputs by regulating the activity of such intervening reticular neurons.

Conclusion

Sensory-driven afferent and propriospinal pathways interact synergistically to enhance the coordination between cervical and lumbar locomotor CPGs of the neonatal rat. Moreover, activation of limb sensory pathways upregulates the discharge of a sub-population of motoneurons, leading to the concomitant production of high frequency action potentials and increased ventral root burst amplitudes. Our results thus show how sensory information is able to influence both local and remote motor outputs in the production of coordinated four-limbed locomotion.

Figure Legends

Figure 1 : Comparison between L-DOPA induced locomotion and air-stepping in the neonatal rat. **A**, Schematic of locomotion recording procedure. **B**, Angular excursions of fore- and hindlimbs of a neonatal rat during L-DOPA induced locomotion. **C**, Same representation as in **A** during air-stepping procedure. **D**, Angular excursions of fore- and hindlimbs of a neonatal rat during L-DOPA induced air-stepping. **E-F**, Bar chart indicating the locomotor movement frequency of the fore- and hindlimbs during locomotion (**E**) and air-stepping (**F**). **G**, Bar chart illustrating the level of coupling between homolateral fore- and hindlimb. **H**, Bar chart illustrating the mean Rayleigh (r) values for the distribution of the homolateral forelimb/hindlimb phase relationships.

Figure 2 : Activation and modulation of fictive locomotion by lumbar dorsal roots stimulation in the isolated brainstem-spinal cord preparation of neonatal rat. **A**, *left*, Schematic of recording/stimulating procedure. ***m****iddle*, Superimposed raw and integrated motor activities recorded from lumbar (left and right L2) and cervical (left and right C8) ventral roots during an episode of alternating bilateral rhythmic stimulation of left and right L2 dorsal roots (stim. L2). *right*, Expanded portion (indicated by dotted lines) of the same traces. **B**, Same representation as in **A** for a preparation that was exposed to a mixture of NMDA (7.5 µM) and 5-HT (15 µM) prior to the dorsal root (DR) stimulation. **C**, Evolution of locomotor burst periods for the preparation in **B**, initially during pharmacological stimulation alone, then during an episode of concomitant DR stimulation. **D**, Same experiment as in **B** showing the evolution of the phase relationships between the cervical extensor-related (right and left C8) and lumbar flexor-related (left L2) activities in relation to right L2 ventral root activity. Sup Th, suprathreshold stimulation.

Figure 3: Long-projection pathway mediating the co-operative influence of lumbar dorsal roots activation on propriospinal lumbo-cervical CPG coupling. **A**, *left*, Schematic of experimental procedure. *Right*, Integrated motor activities recorded in lumbar (left and right L2) and cervical (left and right C8) ventral roots during an episode of subthreshold (Sub Th) alternating bilateral stimulation of left and right L2 DRs (stim. L2). **B**, Suprathreshold enhancement of the locomotor-related ascending drive to the cervical CPGs by low intensity lumbar DR stimulation during selective pharmacological activation of the lumbar CPGs. **B**, *left*, Schematic of experimental procedure. **B**, *right*, Integrated motor activities recorded in lumbar (left and right L2) and cervical (left and right C8) ventral roots during perfusion of NMDA (7.5 µM) and 5-HT (15 µM) over the lumbar segments only, before (left) and during (right) concomitant subthreshold (SubTh) alternating bilateral stimulation of the left and right L2 DRs (stim. L2). During DR stimulation, note the robust activation of the cervical CPGs that were otherwise quiescent, the expression of strictly coordinated cervico-lumbar burst activity and the substantial (~300%) increase in lumbar burst amplitudes. Similar observations were made in 7/7 preparations. **C, D**, Lumbar sensory pathways have direct access to the cervical CPGs. **C**, *left*, Schematic of experimental procedure. **C**, *right*, Integrated motor activities recorded in lumbar (left and right L2) and cervical (left and right C8) ventral roots levels during an episode of low intensity bilateral stimulation of the L2 DRs in combination with application of a subthreshold mixture of NMDA (3.75 µM) and 5-HT (7.5 µM) to the cervical cord region only. Note the activation of the cervical CPG only during additional low intensity lumbar DR stimulation. Similar observations

were made in 9/9 preparations. **D**, *left*, Schematic of experimental procedure in which a subthreshold concentration of NMDA/5-HT was applied selectively to the cervical cord region while the lumbar region was exposed to a low calcium/high magnesium aCSF to block polysynaptic transmission. **D**, *right*, Under these conditions, activation of the cervical CPGs occurred under the additional application of higher levels of lumbar DR stimulation, whereas the lumbar CPGs continued to remain silent. Similar observations were made in 6/7 preparations. **E**, Bar chart indicating the relative threshold required to induce fictive locomotion when stimulating L2 DR, depending on the pharmacological exposure protocol. Note that in the control condition, the locomotor threshold (LocoTh) was found to about twice the minimal stimulation intensity required to trigger a monosynaptic reflex recorded from the ventral root segmental partner of the stimulated dorsal root (see dotted box).

Figure 4: Responses of individual cervical motoneurons to lumbar DR stimulation. **A**, Schematic of experimental procedure. **B**, Antidromic action potentials evoked 1:1 at constant latency in a patch-clamp recorded left C7 motoneuron by single pulse electrical stimulation of the ispilateral C7 ventral root. **C**, Simultaneous recordings of the same C7 motoneuron with indicated cervical and lumbar ventral roots during coordinated locomotor-like activity elicited by suprathreshold (Sup Th) alternating train stimulation of the left and right L2 DRs (stim. L2). **D**, Postsynaptic potentials evoked in a C7 motoneuron by single brief shocks of increasing intensities (0.5-2.5V) applied to the ipsilateral L2 DR. Note the 1:1 occurrence at constant latency of the first post-stimulus EPSP that grades in amplitude with stimulus intensity. **E**, Superimposed traces (in gray) show the EPSP jitter in a C7 motoneuron in response to the stimulation of the ipsilateral L2 DR. Trace in black shows the mean EPSP. **F**, Activity evoked in the same motoneuron in response to alternating bilateral stimulation of left and right L2 DRs (stim. L2) with increasing intensities (0.5-2.5V). Note the depolarization and subthreshold oscillations in the motoneuron's membrane potential even at low DR stimulus intensities, eventually underlying repetitive burst discharge at higher intensities.

Figure 5: Modulation of ongoing fictive locomotion by rhythmic, low intensity lumbar DR stimulation. **A**, *left*, Schematic of experimental procedure. *Right*, Integrated motor activities recorded in lumbar (left and right L2) and cervical (left and right C8) ventral roots during an episode of fictive locomotion induced by the bath application of NMDA (7.5 μM) and 5-HT (15 μM) prior to, and during the same subthreshold intensity of DR stimulation. **B**, Evolution of the locomotor burst periods for the preparation in **A** during NMDA/5-HT stimulation alone, and during concomitant bilateral DR stimulation. **C**, Same preparation showing evolution of the phase relationships between the cervical (right and left C8) and lumbar (left L2) activities relative to right L2. **D**, Wavelet cross coherence between homolateral C8 and L2 ventral root activities (recording in **A)** showing a high coherence (indicated by red coloring) during DR stimulation. **E**, Bar chart illustrating the mean coherence between cervical and lumbar activities under the two indicated experimental conditions (n = 7 preparations). **F**, Instantaneous coherence values throughout the sequence of fictive locomotion shown in **A**. **G**, Mean integrated trace showing the relative increase in rL2 burst amplitude over a single representative cycle during exposure to NMDA/5-HT alone (light blue trace)and during additional subthreshold DR stimulation (dark blue trace. **I**, Group data bar charts (n = 7 preparations) showing the significant (* $p < 0.05$) increase in mean L2R burst amplitude during subthreshold DR stimulation under exposure to NMDA/5-HT.

Figure 6: Comparison between the activity of individual cervical motoneurons during pharmacologically-induced fictive locomotion and in combination with lumbar DR stimulation. **A**, Schematic of experimental procedure. **B**, Sample recording of a C7 motoneuron along with the ipsilateral C7 ventral root and bilateral L2 roots during fictive locomotion induced by NMDA/5HT (left, (1)), and then during an episode of suprathreshold (Sup Th) alternating train stimulation of the bilateral L2 DRs (right, (2)). **C**, Raster plot illustrating the temporal relationship between left C7 motoneuron firing and the mean activity (+/- SEM) of C7 ventral roots (traces at the top), when fictive locomotion was induced by NMDA/5HT. **D**, Circular plots of data from 6 preparations showing the unaltered phase relationships between bursts in individual C7 motoneurons and in different ventral roots during fictive locomotion induced pharmacologically alone (top plot) and in combination with lumbar DR stimulation (bottom plot). **E**, Bar chart showing a >2 fold percentage increase in mean firing frequency during C7 motoneuron bursts under combined pharmacological and dorsal roots stimulation.

Figure 7: Dorsal root stimulation elicits two different discharge responses in cervical motoneurons. **A**, Schematic of experimental procedure. **B**, Example of a C7 motoneuron that fired a single action potential (s.a.Mn; n = 5) in response to single electrical shocks (2.5V, 0.3 ms) applied to the ipsilateral L2 DR. **C**, Cumulative representation of the temporal distribution of single action potentials in s.a.Mn. **D**, **E**, Same representation as in **B**, **C** for a second type of C7 motoneuron that responded with doublet firing (d.a.Mn; n= 5) to the same single stimuli applied to the L2 DR. **F**, Burst activity in a C7 s.a.Mn and in left and right C7 ventral roots during locomotor-like activity evoked by alternating bilateral L2 DR stimulation. **G**, Corresponding plot of instantaneous spike frequency, which displayed a uniform low frequency distribution. **H**, **I**, Graphical representation of the mean firing frequency of C7 s.a.Mn during either pharmacologically (**H**) or CSP (**I**) induced fictive locomotion. Note the absence of doublets in these Mn regardless of the mode of fictive locomotion induction. The dashed line in I indicates the Mn mean frequency during pharmacologically induced fictive locomotion. **J, K**, Same presentation as in **F**, **G** for a C7 d.a.Mn recorded during alternating bilateral L2 DR stimulation. Impulse discharge during bursts was non-uniform (**J**), resulting in two distinct low (blue) and high (green) instantaneous frequency domains (**K**). **L**, Bar chart illustrating the instantaneous frequency values for C7 s.a. and d.a Mns (n = 5 in each case) during sensory pathway-evoked bursting. Note d.a. Mn activity is subdivided into low (blue bar) and high (green bar) frequency bands. **M**, **N**, Same representation as in **H**, **I** for d.a.Mn recorded during either pharmacologically (**M**) or CSP (**N**) induced

fictive locomotion. Note that d.a.Mn show doublets of action potentials only during DR stimulation (**N**) and none during pharmacologically induced locomotion (**M**).

Figure 8: Summary diagram of the convergence of lumbar sensory pathways and propriospinal circuitry between the lumbar and cervical locomotor CPGs. See text for further explanation.

Table 1: Locomotor cycle period variability under the different stimulation methods used for inducing fictive locomotion.

Table 2: Phase relationships between cervical and lumbar ventral root activities under the different stimulation methods used for inducing fictive locomotion.

References

Ampatzis K, Song J, Ausborn J, El Manira A (2014) Separate microcircuit modules of distinct v2a interneurons and motoneurons control the speed of locomotion. Neuron 83:934–943.

Ballion B, Morin D, Viala D (2001) Forelimb locomotor generators and quadrupedal locomotion in the neonatal rat. Eur J Neurosci 14:1727–1738.

Barthélemy D, Leblond H, Provencher J, Rossignol S (2006) Nonlocomotor and locomotor hindlimb responses evoked by electrical microstimulation of the lumbar cord in spinalized cats. J Neurophysiol 96:3273–3292.

Barthélemy D, Leblond H, Rossignol S (2007) Characteristics and mechanisms of locomotion induced by intraspinal microstimulation and dorsal root stimulation in spinal cats. J Neurophysiol 97:1986–2000.

Beliez L, Barrière G, Bertrand SS, Cazalets J-R (2015) Origin of thoracic spinal network activity during locomotor-like activity in the neonatal rat. J Neurosci 35:6117–6130.

Bertrand S, Cazalets JR (1998) Postinhibitory rebound during locomotor-like activity in neonatal rat motoneurons in vitro. J Neurophysiol 79:342–351.

Binder-Macleod S, Kesar T (2005) Catchlike property of skeletal muscle: recent findings and clinical implications. Muscle Nerve 31:681–693.

Burke RE, Rudomin P, Zajac FE (1970) Catch property in single mammalian motor units. Science 168:122–124.

Capogrosso M et al. (2016) A brain-spine interface alleviating gait deficits after spinal cord injury in primates. Nature 539:284–288.

Cazalets JR, Borde M, Clarac F (1995) Localization and organization of the central pattern generator for hindlimb locomotion in newborn rat. J Neurosci 15:4943–4951.

Cazalets JR, Sqalli-Houssaini Y, Clarac F (1992) Activation of the central pattern generators for locomotion by serotonin and excitatory amino acids in neonatal rat. J Physiol 455:187–204.

Denslow JS (1948) Double discharges in human motor units. J Neurophysiol 11:209–215.

Di Prisco GV, Pearlstein E, Robitaille R, Dubuc R (1997) Role of sensory-evoked NMDA plateau potentials in the initiation of locomotion. Science 278:1122–1125.

Dietz V (2002) Do human bipeds use quadrupedal coordination? Trends Neurosci 25:462–467.

Dimitrijevic MR, Gerasimenko Y, Pinter MM (1998) Evidence for a spinal central pattern generator in humans. Ann N Y Acad Sci 860:360–376.

Dose F, Taccola G (2012) Coapplication of noisy patterned electrical stimuli and NMDA plus serotonin facilitates fictive locomotion in the rat spinal cord. J Neurophysiol 108:2977–2990.

Dose F, Zanon P, Coslovich T, Taccola G (2014) Nanomolar oxytocin synergizes with weak electrical afferent stimulation to activate the locomotor CpG of the rat spinal cord in vitro. PLoS One 9:e92967.

Drew T, Rossignol S (1990a) Functional organization within the medullary reticular formation of intact unanesthetized cat. I. Movements evoked by microstimulation. J Neurophysiol 64:767–781.

Drew T, Rossignol S (1990b) Functional organization within the medullary reticular formation of intact unanesthetized cat. II. Electromyographic activity evoked by microstimulation. J Neurophysiol 64:782–795.

Duenas-Jimenez SH, Hernandez LC, Valdovinos B de la T, Ruiz GM, Jimenez JMD, Abundis VR, Garcia IGA (2017) Hind limb motoneurons activity during fictive locomotion or scratching induced by pinna stimulation, serotonin, or glutamic acid in brain cortex-ablated cats. Physiological Reports 5:e13458.

Eccles JC, Hoff HE, Sherrington CS (1932) The rhythmic discharge of motoneurones. Proceedings of the Royal Society of London Series B, Containing Papers of a Biological Character 110:483–514.

English AW (1979) Interlimb coordination during stepping in the cat: an electromyographic analysis. J Neurophysiol 42:229–243.

Fitzgerald M, King AE, Thompson SW, Woolf CJ (1987) The postnatal development of the ventral root reflex in the rat; a comparative in vivo and in vitro study. Neurosci Lett 78:41–45.

Frigon A (2017) The neural control of interlimb coordination during mammalian locomotion. J Neurophysiol 117:2224–2241.

Frigon A, Collins DF, Zehr EP (2004) Effect of rhythmic arm movement on reflexes in the legs: modulation of soleus H-reflexes and somatosensory conditioning. J Neurophysiol 91:1516–1523.

Frigon A, Rossignol S (2006) Experiments and models of sensorimotor interactions during locomotion. Biol Cybern 95:607–627.

Giraudin A, Cabirol-Pol M-J, Simmers J, Morin D (2008) Intercostal and abdominal respiratory motoneurons in the neonatal rat spinal cord: spatiotemporal organization and responses to limb afferent stimulation. J Neurophysiol 99:2626–2640.

Grillner S (1969) The influence of DOPA on the static and the dynamic fusimotor activity to the triceps surae of the spinal cat. Acta Physiol Scand 77:490–509.

Grillner S (2011) Control of Locomotion in Bipeds, Tetrapods, and Fish. In: Comprehensive Physiology, pp 1179–1236. American Cancer Society. Available at: https://onlinelibrary.wiley.com/doi/abs/10.1002/cphy.cp010226 [Accessed June 14, 2021].

Haridas C, Zehr EP, Misiaszek JE (2006) Context-Dependent Modulation of Interlimb Cutaneous Reflexes in Arm Muscles as a Function of Stability Threat During Walking. Journal of Neurophysiology 96:3096–3103.

Hayashi M, Hinckley CA, Driscoll SP, Moore NJ, Levine AJ, Hilde KL, Sharma K, Pfaff SL (2018) Graded Arrays of Spinal and Supraspinal V2a Interneuron Subtypes Underlie Forelimb and Hindlimb Motor Control. Neuron 97:869-884.e5.

Henneman E (1957) Relation between size of neurons and their susceptibility to discharge. Science 126:1345–1347.

Herman R, He J, D'Luzansky S, Willis W, Dilli S (2002) Spinal cord stimulation facilitates functional walking in a chronic, incomplete spinal cord injured. Spinal Cord 40:65–68.

Hiebert GW, Pearson KG (1999) Contribution of sensory feedback to the generation of extensor activity during walking in the decerebrate Cat. J Neurophysiol 81:758–770.

Hiebert GW, Whelan PJ, Prochazka A, Pearson KG (1996) Contribution of hind limb flexor muscle afferents to the timing of phase transitions in the cat step cycle. J Neurophysiol 75:1126–1137.

Hochman S, Schmidt BJ (1998) Whole cell recordings of lumbar motoneurons during locomotor-like activity in the in vitro neonatal rat spinal cord. J Neurophysiol 79:743–752.

Hurteau M-F, Thibaudier Y, Dambreville C, Danner SM, Rybak IA, Frigon A (2018) Intralimb and Interlimb Cutaneous Reflexes during Locomotion in the Intact Cat. J Neurosci 38:4104–4122.

Iizuka M, Kiehn O, Kudo N (1997) Development in neonatal rats of the sensory resetting of the locomotor rhythm induced by NMDA and 5-HT. Exp Brain Res 114:193–204.

Iwahara T, Atsuta Y, Garcia-Rill E, Skinner RD (1991) Locomotion induced by spinal cord stimulation in the neonate rat in vitro. Somatosens Mot Res 8:281–287.

Iwahara T, Atsuta Y, Garcia-Rill E, Skinner RD (1992) Spinal cord stimulation-induced locomotion in the adult cat. Brain Res Bull 28:99–105.

Jankowska E, Jukes MG, Lund S, Lundberg A (1967) The effect of DOPA on the spinal cord. 5. Reciprocal organization of pathways transmitting excitatory action to alpha motoneurones of flexors and extensors. Acta Physiol Scand 70:369–388.

Jordan LM, Schmidt BJ (2002) Propriospinal neurons involved in the control of locomotion: potential targets for repair strategies? Prog Brain Res 137:125–139.

Juvin L, Le Gal J-P, Simmers J, Morin D (2012) Cervicolumbar coordination in mammalian quadrupedal locomotion: role of spinal thoracic circuitry and limb sensory inputs. J Neurosci 32:953–965.

Juvin L, Simmers J, Morin D (2005) Propriospinal circuitry underlying interlimb coordination in mammalian quadrupedal locomotion. J Neurosci 25:6025–6035.

Juvin L, Simmers J, Morin D (2007) Locomotor rhythmogenesis in the isolated rat spinal cord: a phase-coupled set of symmetrical flexion extension oscillators. J Physiol (Lond) 583:115–128.

Kiehn O, Iizuka M, Kudo N (1992) Resetting from low threshold afferents of N-methyl-d-aspartate-induced locomotor rhythm in the isolated spinal cord-hindlimb preparation from newborn rats. Neuroscience Letters 148:43–46.

Kjaerulff O, Kiehn O (1996) Distribution of networks generating and coordinating locomotor activity in the neonatal rat spinal cord in vitro: a lesion study. J Neurosci 16:5777–5794.

Kudina LP, Andreeva RE (2013) Motoneuron double discharges: only one or two different entities? Front Cell Neurosci 7:75.

Kudo N, Yamada T (1987) N-methyl-D,L-aspartate-induced locomotor activity in a spinal cord-hindlimb muscles preparation of the newborn rat studied in vitro. Neurosci Lett 75:43–48.

MacLean JN, Schmidt BJ, Hochman S (1997) NMDA receptor activation triggers voltage oscillations, plateau potentials and bursting in neonatal rat lumbar motoneurons in vitro. Eur J Neurosci 9:2702–2711.

Marchetti C, Beato M, Nistri A (2001) Alternating rhythmic activity induced by dorsal root stimulation in the neonatal rat spinal cord in vitro. J Physiol 530:105–112.

Matsukawa K, Kamei H, Minoda K, Udo M (1982) Interlimb coordination in cat locomotion investigated with perturbation. I. Behavioral and electromyographic study on symmetric limbs of decerebrate and awake walking cats. Exp Brain Res 46:425–437.

Matsuyama K, Drew T (2000) Vestibulospinal and reticulospinal neuronal activity during locomotion in the intact cat. I. Walking on a level surface. J Neurophysiol 84:2237–2256.

McCrea AE, Stehouwer DJ, Van Hartesveldt C (1994) L-dopa-induced air-stepping in preweanling rats. I. Effects of dose and age. Brain Res Dev Brain Res 82:136–142.

McLean DL, Fan J, Higashijima S, Hale ME, Fetcho JR (2007) A topographic map of recruitment in spinal cord. Nature 446:71–75.

Miller S, Van Der Burg J, Van Der Meché F (1975) Coordination of movements of the kindlimbs and forelimbs in different forms of locomotion in normal and decerebrate cats. Brain Res 91:217–237.

Mor Y, Lev-Tov A (2007) Analysis of rhythmic patterns produced by spinal neural networks. J Neurophysiol 98:2807–2817.

Morin D, Viala D (2002) Coordinations of locomotor and respiratory rhythms in vitro are critically dependent on hindlimb sensory inputs. J Neurosci 22:4756–4765.

Mrówczyński W, Celichowski J, Raikova R, Krutki P (2015) Physiological consequences of doublet discharges on motoneuronal firing and motor unit force. Front Cell Neurosci 9:81.

Nakajima T, Mezzarane RA, Klarner T, Barss TS, Hundza SR, Komiyama T, Zehr EP (2013) Neural mechanisms influencing interlimb coordination during locomotion in humans: presynaptic modulation of forearm H-reflexes during leg cycling. PLoS One 8:e76313.

Oueghlani Z, Simonnet C, Cardoit L, Courtand G, Cazalets J-R, Morin D, Juvin L, Barrière G (2018) Brainstem Steering of Locomotor Activity in the Newborn Rat. J Neurosci 38:7725–7740.

Perreault MC, Angel MJ, Guertin P, McCrea DA (1995) Effects of stimulation of hindlimb flexor group II afferents during fictive locomotion in the cat. J Physiol 487:211–220.

Perreault MC, Drew T, Rossignol S (1993) Activity of medullary reticulospinal neurons during fictive locomotion. J Neurophysiol 69:2232–2247.

Perreault MC, Rossignol S, Drew T (1994) Microstimulation of the medullary reticular formation during fictive locomotion. J Neurophysiol 71:229–245.

Phadke CP, Klimstra M, Zehr EP, Thompson FJ, Behrman AL (2010) Soleus h-reflex modulation during stance phase of walking with altered arm swing patterns. Motor Control 14:116–125.

Prochazka A, Gorassini M (1998) Ensemble firing of muscle afferents recorded during normal locomotion in cats. J Physiol 507:293–304.

Reed WR, Shum-Siu A, Onifer SM, Magnuson DSK (2006) Inter-enlargement pathways in the ventrolateral funiculus of the adult rat spinal cord. Neuroscience 142:1195–1207.

Rossignol S (2011) Neural Control of Stereotypic Limb Movements. In: Comprehensive Physiology, pp 173–216. American Cancer Society. Available at: https://onlinelibrary.wiley.com/doi/abs/10.1002/cphy.cp120105 [Accessed July 6, 2021].

Rossignol S, Dubuc R, Gossard J-P (2006) Dynamic sensorimotor interactions in locomotion. Physiol Rev 86:89–154.

Rossignol S, Saltiel P, Perreault M-C, Drew T, Pearson K, Bélanger M (1993) Intralimb and interlimb coordination in the cat during real and fictive rhythmic motor programs. Seminars in Neuroscience 5:67–75.

Ruder L, Takeoka A, Arber S (2016) Long-Distance Descending Spinal Neurons Ensure Quadrupedal Locomotor Stability. Neuron 92:1063–1078.

Schomburg ED, Roesler J, Meinck HM (1977) Phase-dependent transmission in the excitatory propriospinal reflex pathway from forelimb afferents to lumbar motoneurones during fictive locomotion. Neurosci Lett 4:249–252.

Sherrington CS (1910) Flexion-reflex of the limb, crossed extension-reflex, and reflex stepping and standing. J Physiol 40:28–121.

Smith JC, Feldman JL (1987) In vitro brainstem-spinal cord preparations for study of motor systems for mammalian respiration and locomotion. J Neurosci Methods 21:321–333.

Smith JC, Feldman JL, Schmidt BJ (1988) Neural mechanisms generating locomotion studied in mammalian brain stem-spinal cord in vitro. FASEB J 2:2283–2288.

Song J, Dahlberg E, El Manira A (2018) V2a interneuron diversity tailors spinal circuit organization to control the vigor of locomotor movements. Nat Commun 9:3370.

Sqalli-Houssaini Y, Cazalets JR, Clarac F (1993) Oscillatory properties of the central pattern generator for locomotion in neonatal rats. J Neurophysiol 70:803–813.

Taccola G (2011) The locomotor central pattern generator of the rat spinal cord in vitro is optimally activated by noisy dorsal root waveforms. Journal of Neurophysiology 106:872–884.

Taylor A, Durbaba R, Ellaway PH, Rawlinson S (2000) Patterns of fusimotor activity during locomotion in the decerebrate cat deduced from recordings from hindlimb muscle spindles. J Physiol 522:515–532.

Udo M, Kamei H, Matsukawa K, Tanaka K (1982) Interlimb coordination in cat locomotion investigated with perturbation. II. Correlates in neuronal activity of Deiter's cells of decerebrate walking cats. Exp Brain Res 46:438–447.

van den Brand R, Heutschi J, Barraud Q, DiGiovanna J, Bartholdi K, Huerlimann M, Friedli L, Vollenweider I, Moraud EM, Duis S, Dominici N, Micera S, Musienko P, Courtine G (2012) Restoring voluntary control of locomotion after paralyzing spinal cord injury. Science 336:1182–1185.

Viala D, Vidal C (1978) Evidence for distinct spinal locomotion generators supplying respectively fore- and hindlimbs in the rabbit. Brain Res 155:182–186.

Viala G, Buser P (1969) [Stereotyped rhythmic motor activities in the rabbit. A study of their general characteristics]. Exp Brain Res 8:346–363.

Wagner FB et al. (2018) Targeted neurotechnology restores walking in humans with spinal cord injury. Nature 563:65–71.

Wilson DM, Larimer JL (1968) The catch property of ordinary muscle. Proc Natl Acad Sci U S A 61:909–916.

Zajac FE, Young JL (1980) Discharge properties of hindlimb motoneurons in decerebrate cats during locomotion induced by mesencephalic stimulation. Journal of Neurophysiology 43:1221–1235.

Zaporozhets E, Cowley KC, Schmidt BJ (2011) Neurochemical excitation of propriospinal neurons facilitates locomotor command signal transmission in the lesioned spinal cord. J Neurophysiol 105:2818–2829.

Zehr EP, Barss TS, Dragert K, Frigon A, Vasudevan EV, Haridas C, Hundza S, Kaupp C, Klarner T, Klimstra M, Komiyama T, Loadman PM, Mezzarane RA, Nakajima T, Pearcey GEP, Sun Y (2016) Neuromechanical interactions between the limbs during human locomotion: an evolutionary perspective with translation to rehabilitation. Exp Brain Res 234:3059–3081.

Zehr EP, Hundza SR, Vasudevan EV (2009) The quadrupedal nature of human bipedal locomotion. Exerc Sport Sci Rev 37:102–108.

Zehr EP, Klimstra M, Dragert K, Barzi Y, Bowden MG, Javan B, Phadke C (2007) Enhancement of arm and leg locomotor coupling with augmented cutaneous feedback from the hand. J Neurophysiol 98:1810–1814.

Zhong G, Sharma K, Harris-Warrick RM (2011) Frequency-dependent recruitment of V2a interneurons during fictive locomotion in the mouse spinal cord. Nat Commun 2:274.

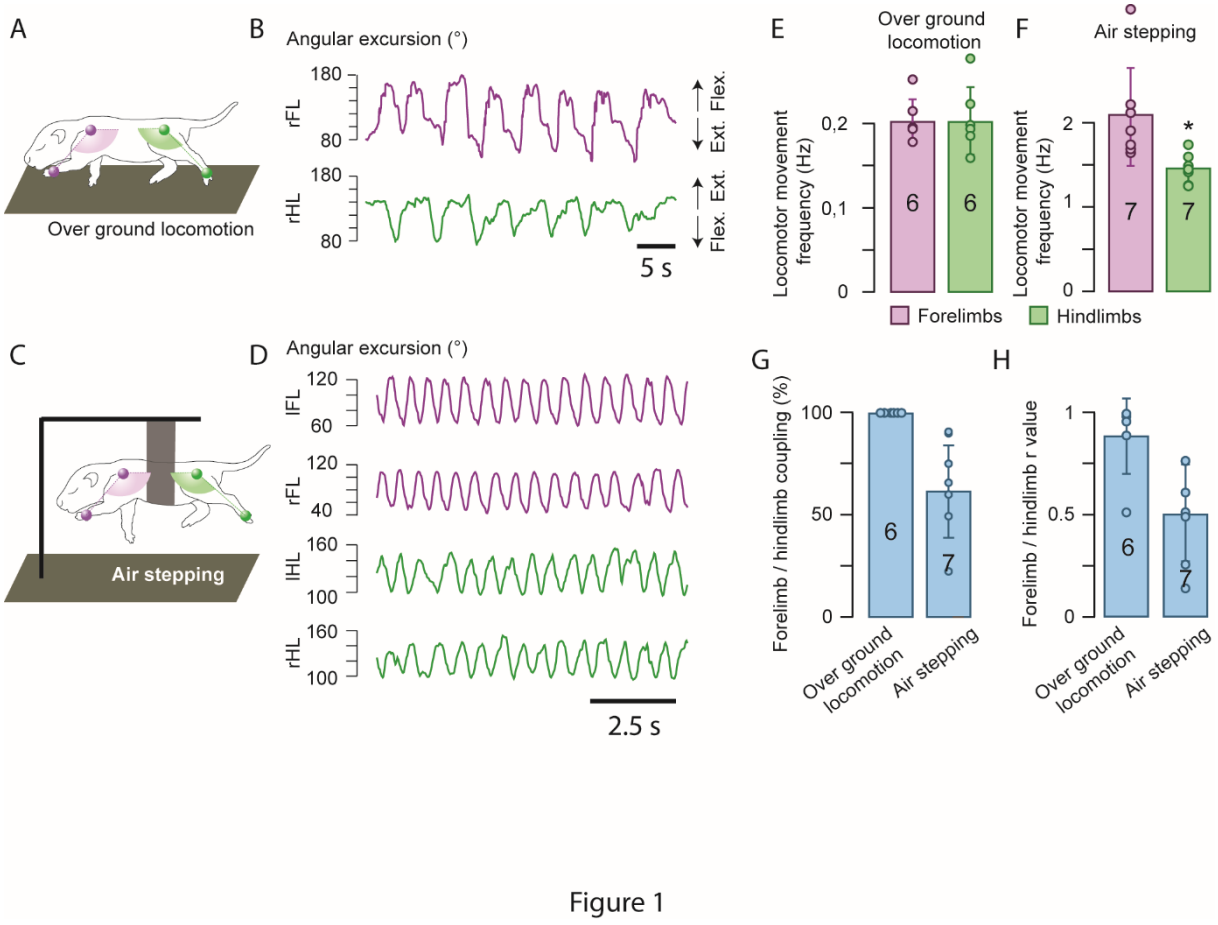
A
B
Angular excursion (°)
Over ground locomotion
rFL
rHL
180
80
Flex.
Ext.
5 s
C
D
Air stepping
lFL
rFL
lHL
rHL
120
60
40
160
100
2.5 s
E
Over ground locomotion
F
Air stepping
Locomotor movement frequency (Hz)
0,2
0,1
0
1
2
6
7
*
Forelimbs
Hindlimbs
G
H
Forelimb / hindlimb coupling (%)
Forelimb / hindlimb r value
100
50
0.5
Over ground locomotion
Air stepping

Figure 1

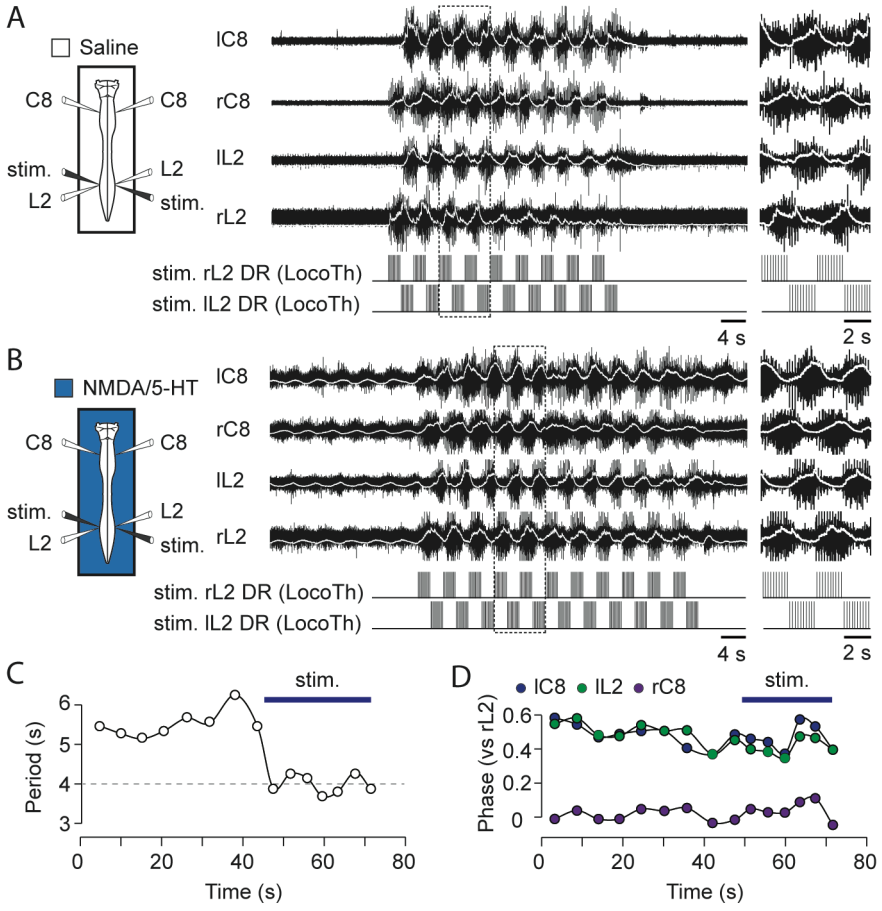
A
Saline
C8
C8
stim.
L2
L2
stim.
lC8
rC8
lL2
rL2
stim. rL2 DR (LocoTh)
stim. lL2 DR (LocoTh)
4 s
2 s
B
NMDA/5-HT
C8
C8
stim.
L2
L2
stim.
lC8
rC8
lL2
rL2
stim. rL2 DR (LocoTh)
stim. lL2 DR (LocoTh)
4 s
2 s
C
stim.
Period (s)
6
5
4
3
0
20
40
60
80
Time (s)
D
lC8
lL2
rC8
stim.
Phase (vs rL2)
0.6
0.4
0.2
0
0
20
40
60
80
Time (s)

Figure 2

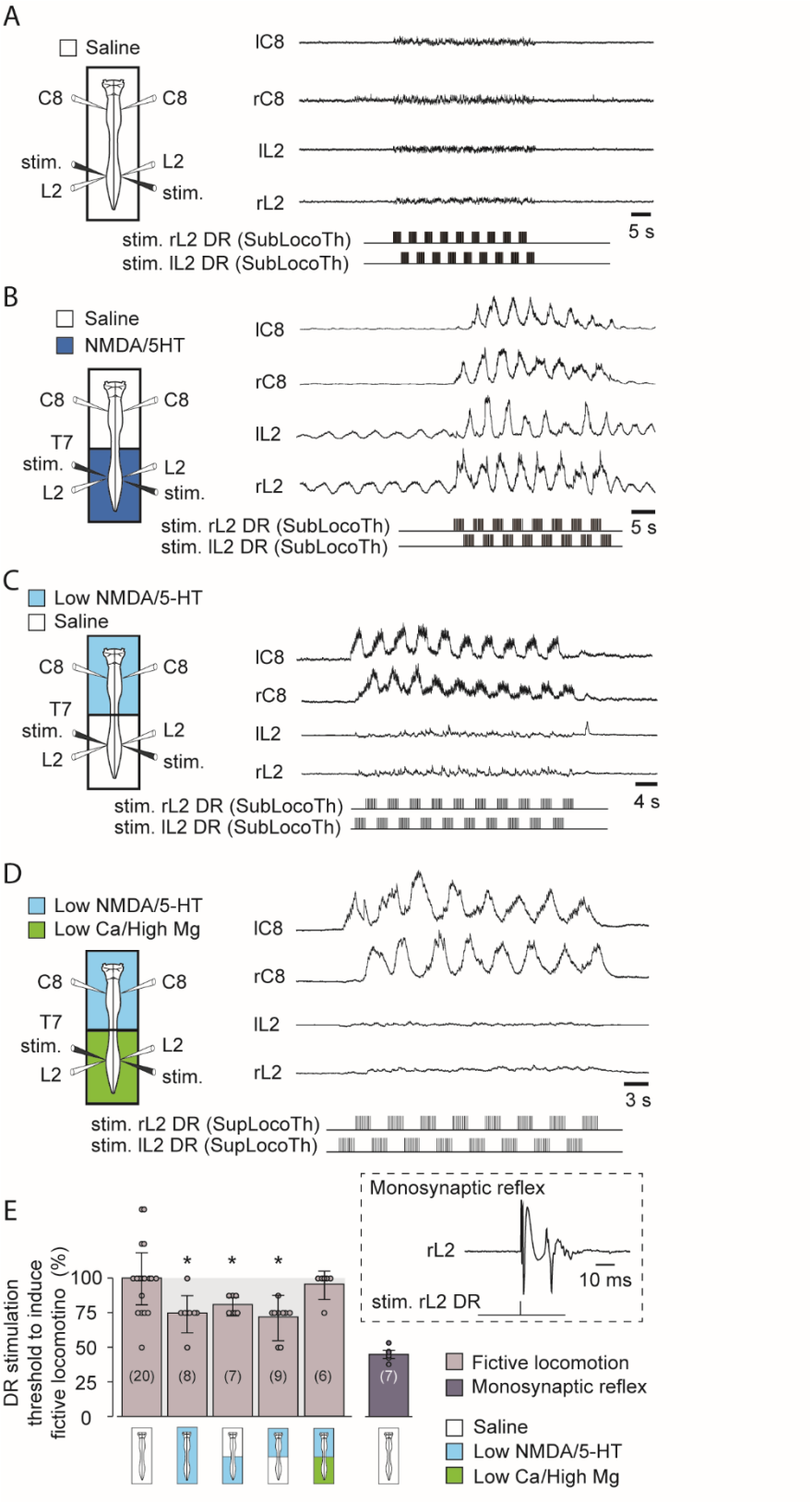
A
Saline
C8
C8
stim.
L2
L2
stim.
lC8
rC8
lL2
rL2
5 s
stim. rL2 DR (SubLocoTh)
stim. lL2 DR (SubLocoTh)
B
Saline
NMDA/5HT
C8
C8
T7
stim.
L2
L2
stim.
lC8
rC8
lL2
rL2
5 s
stim. rL2 DR (SubLocoTh)
stim. lL2 DR (SubLocoTh)
C
Low NMDA/5-HT
Saline
C8
C8
T7
stim.
L2
L2
stim.
lC8
rC8
lL2
rL2
4 s
stim. rL2 DR (SubLocoTh)
stim. lL2 DR (SubLocoTh)
D
Low NMDA/5-HT
Low Ca/High Mg
C8
C8
T7
stim.
L2
L2
stim.
lC8
rC8
lL2
rL2
3 s
stim. rL2 DR (SupLocoTh)
stim. lL2 DR (SupLocoTh)
E
DR stimulation threshold to induce fictive locomotino (%)
100
75
50
25
0
(20)
(8)
(7)
(9)
(6)
(7)
Monosynaptic reflex
rL2
10 ms
stim. rL2 DR
Fictive locomotion
Monosynaptic reflex
Saline
Low NMDA/5-HT
Low Ca/High Mg

Figure 3

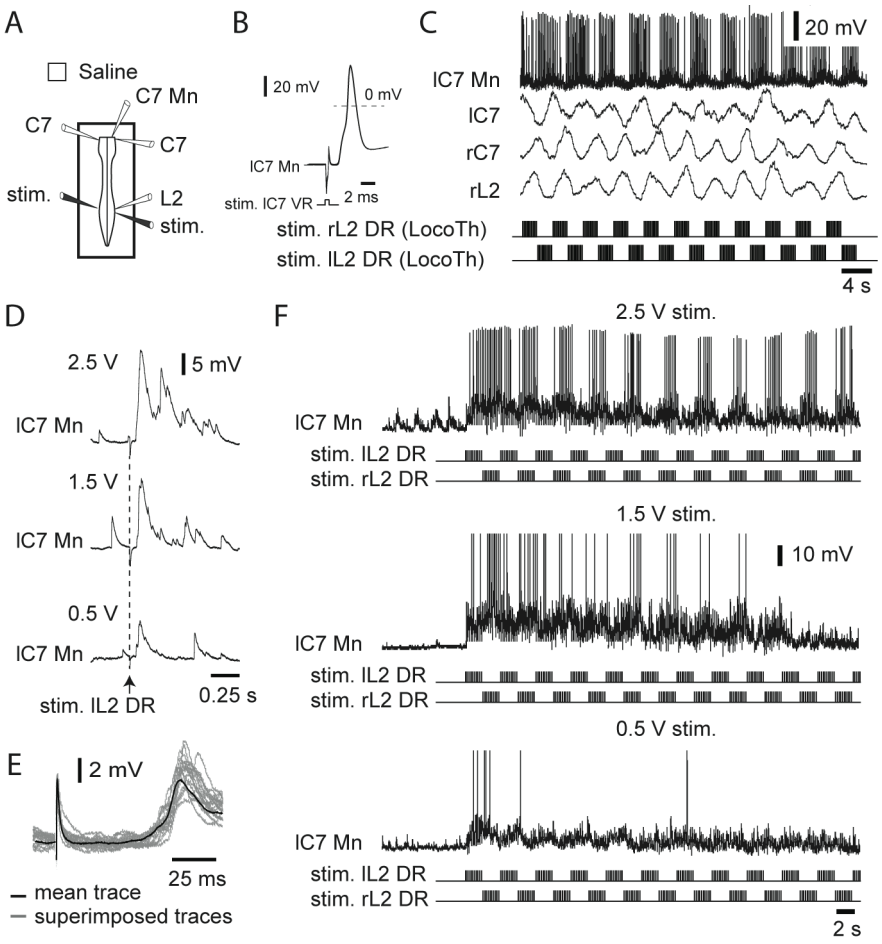
A
Saline
C7 Mn
C7
C7
stim.
L2
stim.
B
20 mV
0 mV
IC7 Mn
stim. IC7 VR
2 ms
C
20 mV
IC7 Mn
IC7
rC7
rL2
stim. rL2 DR (LocoTh)
stim. IL2 DR (LocoTh)
4 s
D
2.5 V
5 mV
IC7 Mn
1.5 V
IC7 Mn
0.5 V
IC7 Mn
stim. IL2 DR
0.25 s
E
2 mV
25 ms
mean trace
superimposed traces
F
2.5 V stim.
IC7 Mn
stim. IL2 DR
stim. rL2 DR
1.5 V stim.
10 mV
IC7 Mn
stim. IL2 DR
stim. rL2 DR
0.5 V stim.
IC7 Mn
stim. IL2 DR
stim. rL2 DR
2 s

Figure 4

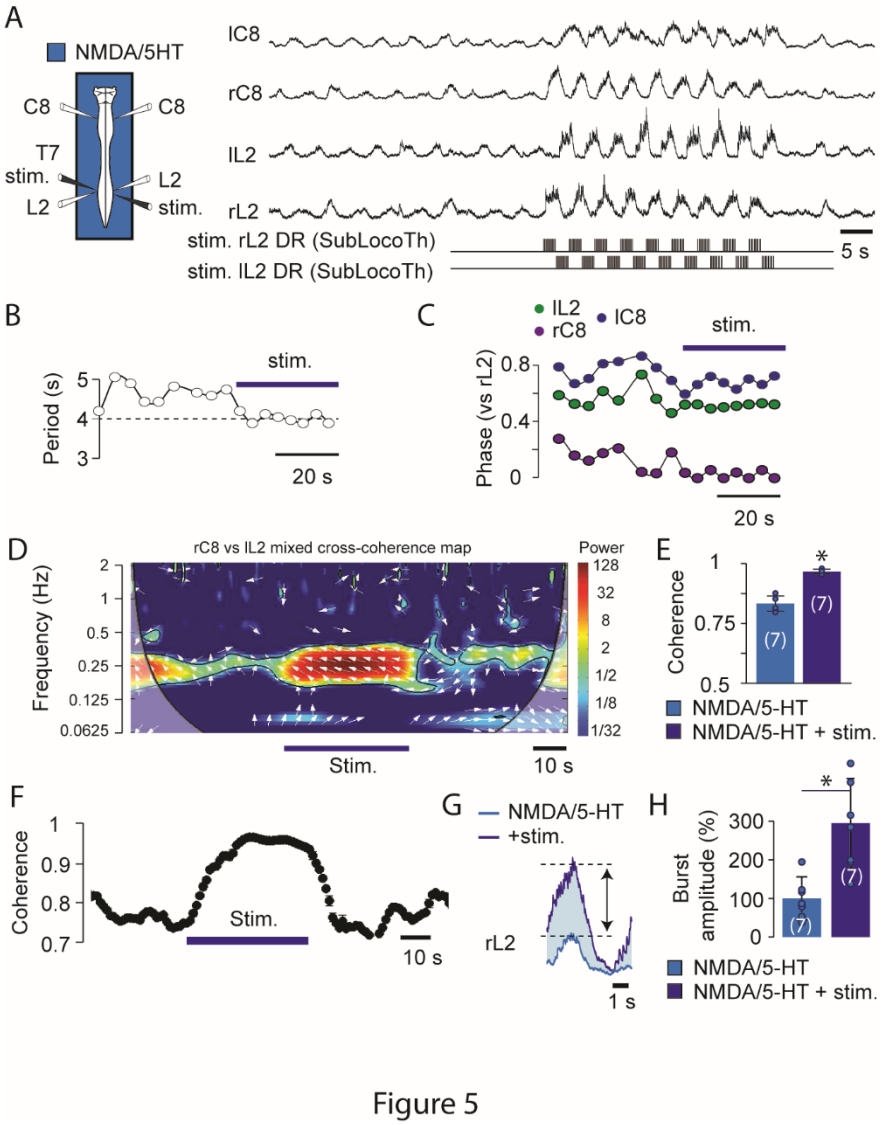
A
NMDA/5HT
C8
C8
T7
stim.
L2
L2
stim.
IC8
rC8
IL2
rL2
stim. rL2 DR (SubLocoTh)
stim. IL2 DR (SubLocoTh)
5 s
B
Period (s)
stim.
20 s
C
IL2
rC8
IC8
stim.
Phase (vs rL2)
20 s
D
rC8 vs IL2 mixed cross-coherence map
Power
Frequency (Hz)
Stim.
10 s
E
Coherence
(7)
(7)
NMDA/5-HT
NMDA/5-HT + stim.
F
Coherence
Stim.
10 s
G
NMDA/5-HT
+stim.
rL2
1 s
H
Burst amplitude (%)
(7)
(7)
NMDA/5-HT
NMDA/5-HT + stim.

Figure 5

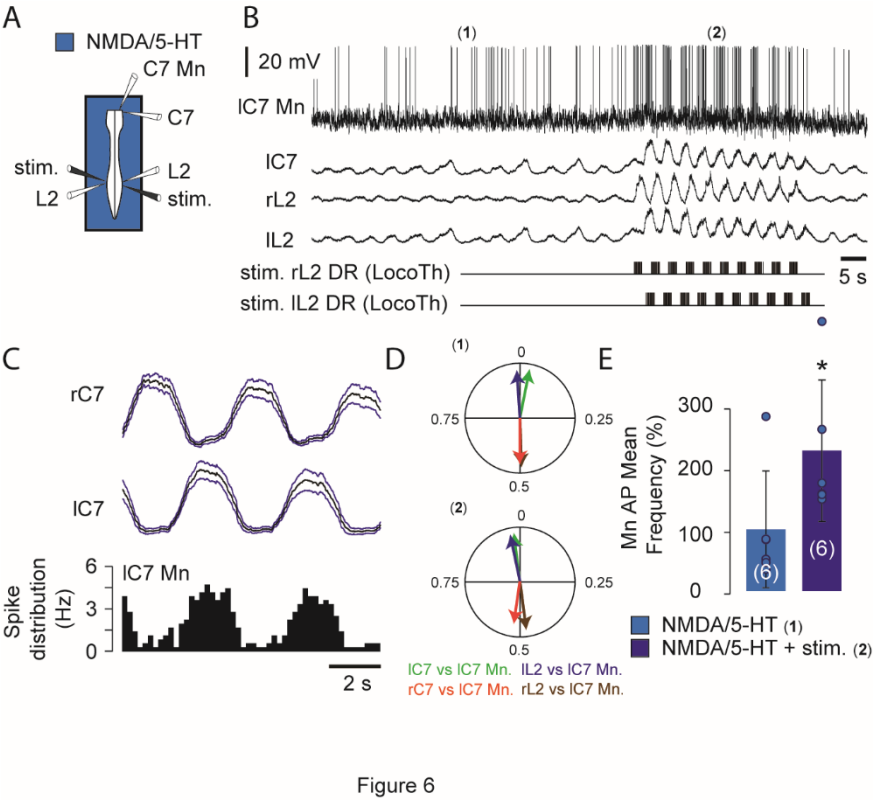
A
NMDA/5-HT
C7 Mn
C7
stim.
L2
L2
stim.
B
(1)
(2)
20 mV
IC7 Mn
IC7
rL2
lL2
stim. rL2 DR (LocoTh)
stim. lL2 DR (LocoTh)
5 s
C
rC7
IC7
Spike distribution (Hz)
6
3
0
IC7 Mn
2 s
D
(1)
(2)
0
0.25
0.5
0.75
IC7 vs IC7 Mn.
lL2 vs IC7 Mn.
rC7 vs IC7 Mn.
rL2 vs IC7 Mn.
E
Mn AP Mean Frequency (%)
300
200
100
0
*
(6)
(6)
NMDA/5-HT (1)
NMDA/5-HT + stim. (2)

Figure 6

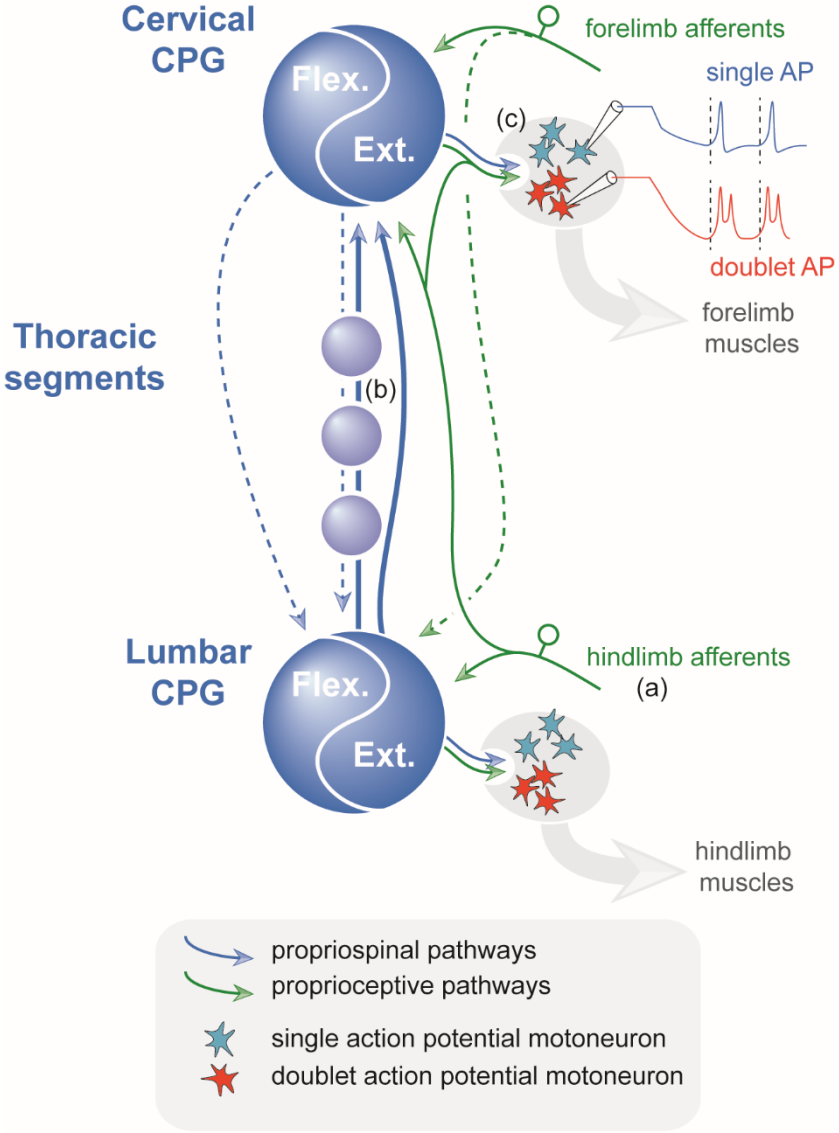
Cervical CPG
Flex.
Ext.
forelimb afferents
single AP
(c)
doublet AP
forelimb muscles
Thoracic segments
(b)
Lumbar CPG
Flex.
Ext.
hindlimb afferents
(a)
hindlimb muscles
propriospinal pathways
proprioceptive pathways
single action potential motoneuron
doublet action potential motoneuron

Figure 8

Condition	T (s) (+/- SD)	p (ANOVA)	F (6, 48)	p (Tukey)*	n	CV	
NMA/5HT Prep	5.13 +/- 1.05	*<0.001*	*5,57*	*NA*	*9*	0,20	*Fig. 2*
NMA/5HT Prep + Stim (Th)	3.98 +/- 0.06	*<0.001*	*5,57*	*0.002*	*9*	0,02	
NMA/5HT Prep + Stim (SubTh)	4.04 +/- 0.35	*<0.001*	*5,57*	*0.039*	*7*	0,09	*Not shown*
NMA/5HT Lomb	4.75 +/- 1.00	*<0.001*	*5,57*	*0.849*	*7*	0,21	
NMA/5HT Lomb + Stim (SubTh)	4.00 +/- 0.13	*<0.001*	*5,57*	*0.014*	*7*	0,03	*Fig. 3*
low NMA/5HT Prep + Stim (SubTh)	3.98 +/- 0.03	*<0.001*	*5,57*	*0.003*	*8*	0,01	
low NMA/5HT Lomb + Stim (SubTh)	3.97 +/- 0.03	*<0.001*	*5,57*	*0.004*	*7*	0,01	

*T vs $T_{NMA/5HT\ Prep}$

Table 1

	Phase /rL2										
Condition	rC8	p (ANOVA on ranks)	H (5, 45)	lC8	p (ANOVA on ranks)	H (5, 45)	lL2	p (ANOVA on ranks)	H (6, 54)	n	
NMA/5HT Prep	0.05 +/- 0.07	*0.275*	*6,33*	0.58 +/- 0.08	*0.914*	*1,49*	0.54 +/- 0.04	*0.133*	*9,81*	*9*	*Fig. 2*
NMA/5HT Prep + Stim (Th)	0.06 +/- 0.03	*0.275*	*6,33*	0.55 +/- 0.09	*0.914*	*1,49*	0.50 +/- 0.06	*0.133*	*9,81*	*9*	
NMA/5HT Prep + Stim (SubTh)	0.05 +/- 0.02	*0.275*	*6,33*	0.57 +/- 0.13	*0.914*	*1,49*	0.54 +/- 0.02	*0.133*	*9,81*	*7*	*Not shown*
NMA/5HT Lomb	*NA*	*NA*	*NA*	*NA*	*NA*	*NA*	0.49 +/- 0.06	*0.133*	*9,81*	*7*	
NMA/5HT Lomb + Stim (SubTh)	0.04 +/- 0.02	*0.275*	*6,33*	0.53 +/- 0.09	*0.914*	*1,49*	0.49 +/- 0.07	*0.133*	*9,81*	*7*	*Fig. 3*
low NMA/5HT Prep + Stim (SubTh)	0.02 +/- 0.05	*0.275*	*6,33*	0.57 +/- 0.04	*0.914*	*1,49*	0.57 +/- 0.05	*0.133*	*9,81*	*8*	
low NMA/5HT Lomb + Stim (SubTh)	0.02 +/- 0.02	*0.275*	*6,33*	0.56 +/- 0.09	*0.914*	*1,49*	0.54 +/- 0.08	*0.133*	*9,81*	*7*	

Table 2